1996 JANNAF Propulsion Systems Hazards Subcommittee Meeting, Naval Postgraduate School, Monterey, CA (4-8 Nov 96)

A Global HMX Decomposition Model*

M. L. Hobbs

Sandia National Laboratories, Albuquerque, New Mexico 87185†

ABSTRACT

HMX (octahydro-1,3,5,7-tetranitro-1,3,5,7-tetrazocine) decomposes by competing reaction pathways to form various condensed and gas-phase intermediate and final products. Gas formation is related to the development of nonuniform porosity and high specific surface areas prior to ignition in cookoff events. Such thermal damage enhances shock sensitivity and favors self-supported accelerated burning. The extent of HMX decomposition in highly confined cookoff experiments remains a major unsolved experimental and modeling problem. The present work is directed at determination of global HMX kinetics useful for predicting the elapsed time to thermal runaway (ignition) and the extent of decomposition at ignition.

Kinetic rate constants for a six step engineering based global mechanism were obtained using gas formation rates measured by Behrens[1] at Sandia National Laboratories with his Simultaneous Modulated Beam Mass Spectrometer (STMBMS) experimental apparatus. The six step global mechanism includes competition between light gas (H_2O, HCN, CO, H_2CO, NO, N_2O) and heavy gas ($C_2H_6N_2O$ and $C_4H_{10}NO_2$) formation with zero order sublimation of HMX and the mononitroso analog of HMX (mn-HMX), $C_4H_8N_8O_7$. The global mechanism was applied to the highly confined, One Dimensional Time to eXplosion (ODTX) experiment[2] and hot cell experiment[3] by suppressing the sublimation of HMX and mn-HMX. An additional gas-phase reaction was also included to account for the gas-phase reaction of N_2O with H_2CO. Predictions compare adequately to the STMBMS data, ODTX data, and hot cell data. Deficiencies in the model and future directions are discussed.

INTRODUCTION

Heated energetic materials develop nonuniform porosities and high specific surface areas prior to ignition in cookoff events.[4] Such thermal damage, created by various chemical and physical processes, enhances shock sensitivity and favors self-supported accelerated combustion.[5] Following ignition, the subsequent level of violence depends on the competition between dynamic pressure buildup and stress release due to loss of confinement. Predictive capability within Sandia National Laboratories Engineering Sciences Center is being developed to determine the level of violence ranging from a mild pressure burst to a detonation. The present work is aimed at predicting the path dependent extent of reaction of HMX which is needed to determine porosity and specific surface area at ignition. The porosity and specific surface area of the HMX at ignition become the initial condition for subsequent dynamic analysis.

A commonly used HMX decomposition mechanism applied to cookoff analysis is the three step global mechanism developed at Lawrence Livermore National Laboratories (LLNL) by Tarver et al.[2] based on ODTX experiments:

$$HMX \xrightarrow{1} fragments \xrightarrow{2} intermediate\ gases \xrightarrow{3} final\ gases \qquad (1)$$

$$C_4H_8N_8O_8 \quad CH_2NNO_2 \quad CH_2O, N_2O, HCN, HNO_2 \quad N_2, H_2O, CO_2, CO$$

The activation energy for the initial endothermic unimolecular bond-breaking reactions was obtained from the weakly confined Henkin test; the activation energy of the second mildly exothermic unimolecular reaction was reported to be consistent with intermediate confinement tests; and the activation energy of the final highly exothermic bimolecular reaction was based on measured gas-phase kinetics. The number of moles of gas produced by each of the global reaction steps in Eq. (1) was not reported.

The temporal behavior of the rates of formation of HMX decomposition gases were measured by Behrens[1] in Sandia National Laboratories' Simultaneous Modulated Beam Mass Spectrometer (STMBMS) experimental apparatus. Behrens concluded that complex physical processes and chemical mechanisms within the condensed phase controlled the HMX decomposition. Recently, Behrens and Bulusu[6] gave a qualitative model of the physical and chemical processes that control decomposition of HMX in the solid phase: 1) HMX initially decomposes to the mononitroso analog of HMX (mn-HMX) at individual lattice sites within the particles, 2) mn-HMX decomposes to gaseous products forming bubbles within the lattice, 3) the gaseous products move within and interact with the lattice, 4) the weakened lattice forms HCN from the ring and HONO with associated decomposition products, 5) mn-HMX continues to decom-

*Approved for public release; distribution is unlimited

†This work performed at Sandia National Laboratories supported by the U.S. Department of Energy under contract DE-AC04-94AL85000.

pose to gaseous products as well as a nonvolatile product which eventually becomes unstable and decomposes to formamides and dimethylnitrosamine, 6) growing bubbles physically crack the HMX particles and release gaseous products, 7) gaseous products interact with the remaining HMX and accelerate decomposition, 8) the HMX is depleted and a residue with polyamide characteristics remains. The pressure within the STMBMS reaction vessel is only about 1 torr. The formation of decomposition products within the solid HMX are likely at pressures greater than 1 atm. Behrens postulates the pressure within the bubbles to be between 10 and 100 atm by assuming 5 μm bubbles with reasonable surface tensions.[7]

The STMBMS apparatus detects the rate of formation of HMX decomposition gases and does not directly give data on condensed phase products. Condensed phase products are not treated explicitly in the present paper. Rather, a simple global mechanism is presented that predicts gas formation rates only. Arrhenius rate constants and reaction order are obtained using the DAKOTA (Design Analysis Kit for OpTimizAtion) toolkit.[8] The simple global mechanism is applied to the highly confined ODTX and hot cell experiments by restricting the sublimation reactions and adding a second order gas-phase reaction.

STMBMS HMX DATA

Fig. 1 illustrates the time resolved distribution of HMX decomposition products measured at three different temperatures by Behrens.[1] The gaseous decomposition products are: 1) HMX, 2) mn-HMX, 3) N_2O, 4) CH_2O, 5) H_2O, 6) NO, 7) CO/N_2, 8) HCN, 9) $C_2H_6N_2O$ and 10) $C_4H_{10}N_2O_2$. The gaseous products are detected with a mass spectrometer and provide a direct measure of the gas formation rates within the reaction cell. The reactive gases, N_2O and H_2CO, are expected to react exothermically with higher levels of confinement. However, this gas-phase reaction will not be considered until the mechanism is applied to confined systems.

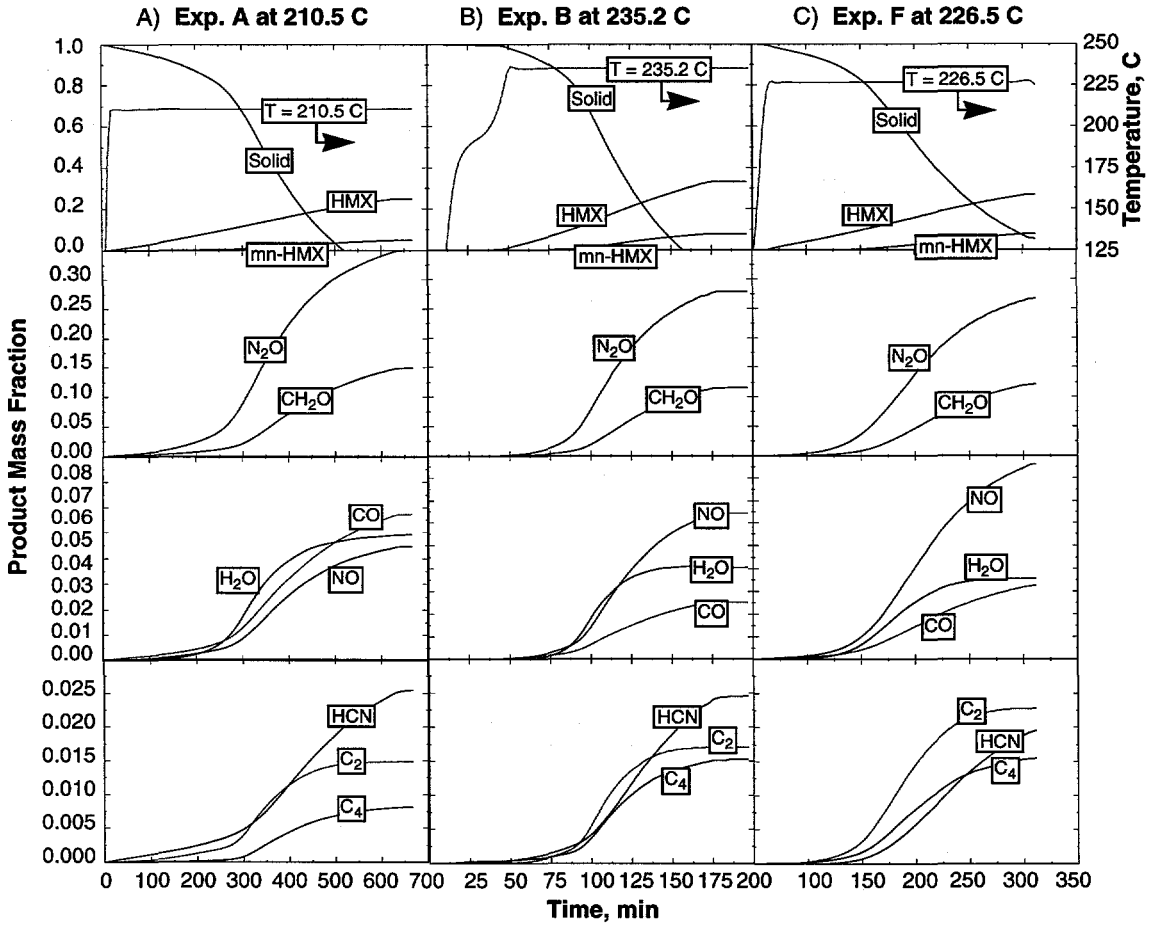

Fig. 1. Measured[1] HMX decomposition products at A) 210.5 C, B) 235.2 C, and C) 226.5 C. mn-HMX, C_2, C_4 represent the mononitroso analog of HMX, dimethlynitrosamine ($C_2H_6N_2O$), and an amide species ($C_4H_{10}N_2O_2$), respectively.

DISCLAIMER

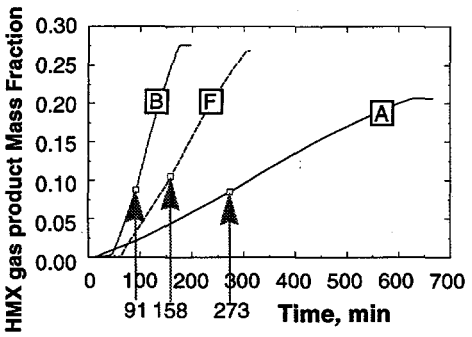

Fig. 2. HMX (gas) product mass fraction for experiments A, B, and F. The squares are located near slope changes.

A striking feature of all decomposition gases shown in Fig. 1 is the abrupt change in reactivity near 91 min., 158 min., and 273 min. for experiment B, F, and A, respectively. This change is depicted in the HMX gaseous product mass fractions as plotted in Fig. 2. Although HMX sublimation is expected to be linear throughout the STMBMS experiment, a change in slope is apparent for each experiment in Fig. 2. The change in slope shown in Fig. 2 may be a result of a physical change such as the solid-to-solid HMX phase transition which creates reactive sites that enhance reactivity. Details regarding phase transformations are discussed more fully in a companion paper at this PSHS meeting.[4]

The sublimation rate is expected to remain constant if the surface of the HMX particles remains the same. However, the sublimation pressure changes as the energy associated with surface bonding changes. The mechanism in the present paper is based on the decomposition process following the slope change, as shown in Fig. 2, where most of the decomposition occurs.

Other notable observations from the measured HMX decomposition product distributions are: 1) H_2O formation rates are maximum when N_2O rates are maximum, 2) CH_2O, NO, CO/N_2 have similar temporal behavior, 3) dimethlynitrosamine ($C_2H_6N_2O$) formation rates are maximum when the amide species ($C_4H_{10}N_2O_2$) formation rates are maximum, and 4) HCN formation rates are maximum when the mn-HMX formation rates are maximum. Formation rates are plotted in Ref. 1.

GLOBAL HMX MECHANISM

The global HMX mechanism is based on temporally correlated reaction product formation rates. For example, zero order sublimation reactions describe the formation of HMX and mn-HMX. Formation of H_2O is assumed to be correlated with the formation of N_2O. The following stoichiometrically balanced six step global mechanism can be used to predict the HMX decomposition species measured by Behrens[1] as a function of temperature history:

$$HMX^c \rightarrow HMX^g \quad \text{(R-1)}$$

$$HMX^c \rightarrow 4\,N_2O^g + 4\,H_2O^g + C_4^c \quad \text{(R-2)}$$

$$HMX^c \rightarrow \text{mn-}HMX^g + O^c \quad \text{(R-3)}$$

$$HMX^c \rightarrow 4\,N_2O^g + 4\,H_2CO^g \quad \text{(R-4)}$$

$$HMX^c + H_2CO^g \rightarrow C_2H_6N_2O^g + 3\,CO^g + 5\,NO^g + NH_4^c \quad \text{(R-5)}$$

$$HMX^c + 2\,H_2CO^g \rightarrow C_4H_{10}N_2O_2{}^g + 2\,HCN^g + 4\,NO^g + O_4^c \quad \text{(R-6)}$$

where the superscript c and g represent condensed-phase and gas-phase, respectively. The species C_4, O, NH_4, and O_4 are assumed to be nonvolatile and remain in the solid residue. Reaction (R-4) was chosen as the primary source of H_2CO which subsequently reacts with HMX to form the dimethylnitrosamine and amide product.

SPECIES RATE EQUATIONS

For each global reaction step j, the reaction rate, r_j, is assumed to be described by:

$$r_j = k_j(T)[HMX]^{n_j}, \quad j = 1, \ldots 6 \quad (2)$$

where k, T, $[HMX]$, and n represent the Arrhenius rate coefficient (1/s-mole^{n-1}), temperature (K), moles of HMX, and reaction order, respectively. The global reaction rates r_5 and r_6 are only based on the moles of HMX as discussed in the **KINETIC RATE PARAMETER** section. Global rate dependence on the moles of H_2CO for r_5 and r_6 was found to be negligible. The expressions for the kinetic coefficients, $k_j(T)$, are given in an Arrhenius form:

$$k_j(T) = A_j exp(-E_j/RT) \quad (3)$$

where A_j (1/s), E_j (cal/mol), and R (1.987 cal/mol-K) are the pre-exponential factors, activation energies, and the universal gas constant, respectively. The rates of change of species are given by:

$$dN_i/dt = \sum_{j=1}^{6} \nu_{ij} r_j \quad , \qquad i = 1, \ldots 15 \tag{4}$$

where N_i, t, ν_{ij} are the concentration of species i (moles), time (sec), and the stoichiometric coefficients of the i^{th} species in the j^{th} reaction, respectively. Fifteen species are considered in the global mechanism. The parameters needed for the global mechanism are A_j, E_j, and n_j.

KINETIC RATE PARAMETERS

The HMX mechanism is based on the data which follows the slope change as discussed in the **STMBMS HMX DATA** section. The species rate equations represent an initial value problem with the initial value set to the mole fraction at 91 min., 158 min., and 273 min. for experiment B, F, and A, respectively. For convenience, the initial time for each experiment was reset to zero. The initial species mole fractions are given in Table 1. The temperature for each experiment was held constant at 210.5 C, 235.2 C, and 226.5 C for experiment A, B, and F, respectively.

TREX[9] was chosen as the analysis code to solve the initial value problem. Starting with reasonable values for the kinetic rate parameters (A_j, E_j, and n_j) an objective function was minimized using DAKOTA[8] (Design Analysis Kit for OpTimizAtion). The objective function was the normalized squared difference between calculated and measured product distributions for Behren's experiment A, B, and F:

$$error = \sum_{k}^{3} \sum_{i}^{11} \left[\frac{N_{i,k}^{calc} - N_{i,k}^{meas}}{N_{i,k}^{meas}} \right]^2 \tag{5}$$

where the superscripts *calc* and *meas* represent calculated and measured product mole fractions, respectively. The subscripts k and i represent the three STMBMS experiments and the number of species, respectively. Fig. 3 shows the conceptualized TREX interface with the DAKOTA[8] toolkit which utilizes object-oriented design to interface analysis codes to various optimization techniques. The input deck generator is based on an algebraic preprocessor, APREPRO.[10] The error calculator is a FORTRAN code used to read TREX output and compute the error function given in Eq. (5). The input generator and error calculator are controlled by a C-shell script.

Table 1. Initial mole fractions for HMX experiments*

Species	Exp. A	Exp. B	Exp. F
1 - H_2O	0.1018	0.09268	0.08817
2 - HCN	0.02324	0.01942	0.007612
3 - CO	0.05812	0.02562	0.03346
4 - H_2CO	0.08011	0.06360	0.07246
5 - NO	0.03473	0.04691	0.07708
6 - N_2O	0.2132	0.1751	0.1904
7 - $C_2H_6N_2O$	0.005429	0.006769	0.01098
8 - $C_4H_{10}N_2O_2$	0.0005390	0.003094	0.003551
9 - mn-HMX	0.002472	0.003366	0.004306
10 - HMX gas	0.04610	0.05407	0.06016
11 - HMX solid	0.4343	0.5094	0.4518

*The initial values for C_4, O, NH_4, and O_4 were assumed to be 0.0.

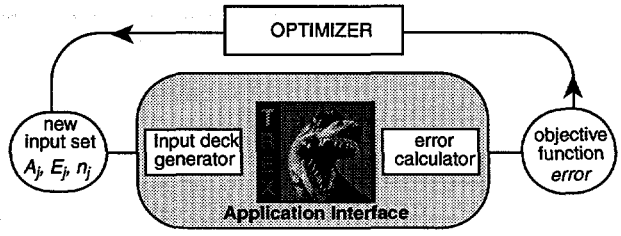

Fig. 3. TREX interface with DAKOTA.

The N-N bond is the weakest covalent bond in the HMX molecule with an estimated bond energy of 40 kcal/mole.[12] A lower bound on the apparent activation energy for each global reaction step in the current paper was chosen as 36 kcal/mole in order to enforce reasonable values of activation energy. Lower apparent activation energies are probably acceptable since the rate limiting process may be a physical process rather than a chemical process. Reaction orders were chosen to be near unity except for the HMX sublimation reaction (R-1) and the mn-HMX sublimation reaction (R-3). The orders of the sublimation reactions were assumed to be 0-order.

The values of the 18 parameters, A_j, E_j, and n_j, were determined by minimizing the error shown in Eq (5). All parameters could not be minimized simultaneously because of the greater sensitivity of the Arrhenius parameters than the reaction orders. The parameter optimization proceeded as follows:

1) n_1 and n_3 set to 0, all remaining orders set to 1.

2) Optimizer used to determine A_1, A_3, E_1, and E_3 for (R-1) and (R-3).

3) Optimizer used to determine A_2 and E_2 by weighting the error for the H_2O concentrations.

Table 2. Optimized Parameters for reactions R-1 through R-6

Rxn	Order	Ln A	E/R, K	h_{rxn}, cal/g
R-1	0	29.1	20230	-141.4
R-2	0.85 in HMX	28.2	18900	+577.0
R-3	0	28.9	20670	0.0
R-4	1.07 in HMX	27.0	18000	+170.0
R-5	0.84 in HMX	27.1	18700	0.0
R-6	0.91in HMX	25.5	18600	0.0
R-7*	1 in N_2O, 1 in H_2CO	28.1	17170	+1200

*Parameters for (R-7) were obtained from Ref. (2) rather than by optimization. Discussion of (R-7) is given in the **MODEL APPLICATION** section.

4) Optimizer used to determine A_4 and E_4 by weighting the error for the N_2O concentrations.

5) Optimizer used to determine A_5, A_6, E_5, and E_6.

6) Optimizer used to determine n_2, n_4, n_5, and n_6.

The optimized parameters are given in Table 2. The model and experimental results are shown in Fig. 4. Comparisons between model and data can be made in general by looking at the solid product mass fraction. The computed solid mass fraction is generally higher than measure values for Exp. A and lower than measured values for Exp. B and Exp. C. The largest percent difference between model and data are probably for the HCN. Other reaction paths for HCN exist as discussed by Behrens and Bulusu.[6] However, additional reactions to account for HCN production did not seem warranted for this global reaction since measured HCN production was relatively low.

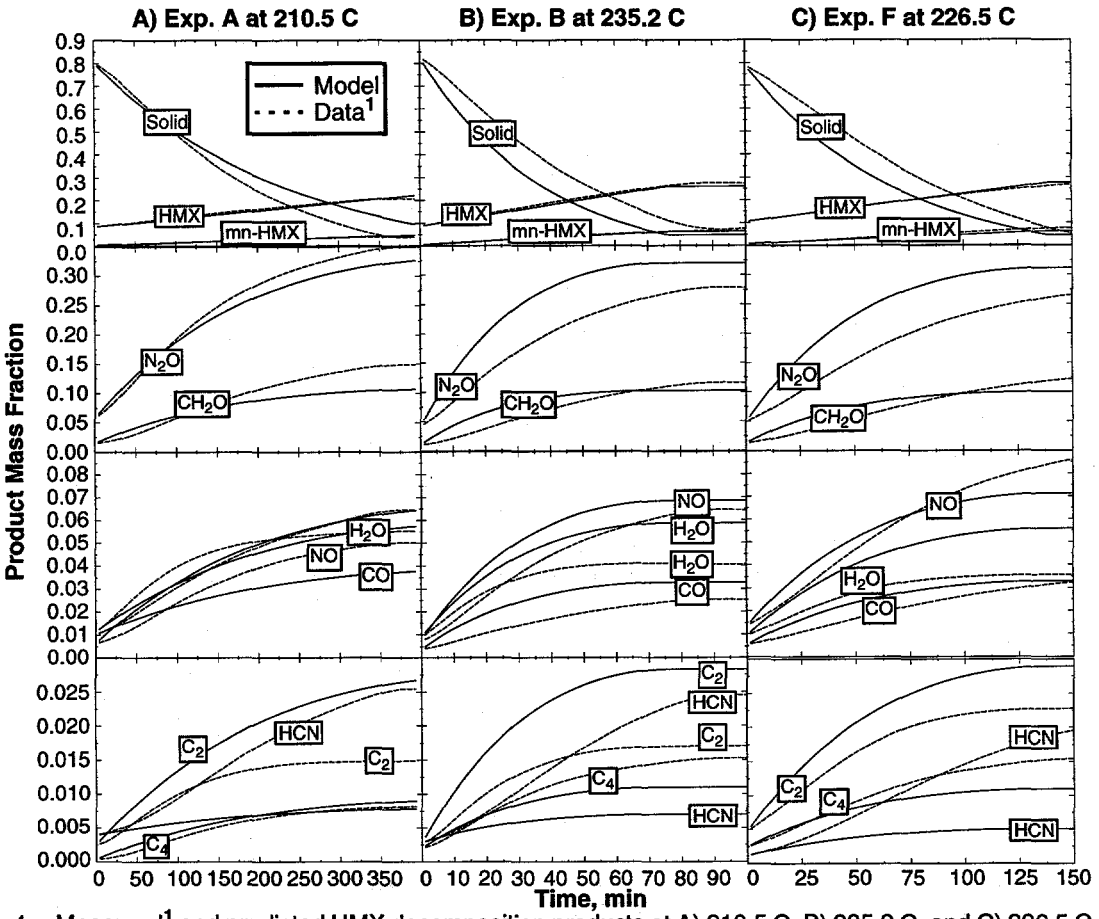

Fig. 4. Measured[1] and predicted HMX decomposition products at A) 210.5 C, B) 235.2 C, and C) 226.5 C. Initial concentrations based on values given in Table 1. Predicted values based on (R-1) through (R-6) with kinetic parameters reported in Table 2.

MODEL APPLICATION

The global HMX mechanism has been applied to several cookoff experiments. The cookoff experiments chosen for simulation are for confined systems. Typically, the One Dimensional Time to eXplosion (ODTX) experiments[2] are confined to 1500 atm; and the hot cell experiments[3] are confined at 600 atm. The STMBMS experiments is oper-

ated near vacuum and the HMX decomposition products exit the reaction vessel without reacting substantially in the gas-phase. The sublimation reactions (R-1) and (R-3) are suppressed to account for the high pressure. Gas-phase reactions are also required to account for gas-phase interactions in the highly confined systems. Tarver and McGuire[2] give the average activation energy for these gas-phase reactions as 34 kcal/mol. The following reaction between the major gas-phase species is assumed to describe all gas-phase reactions:

$$N_2O + H_2CO \rightarrow H_2O + N_2 + CO \qquad \text{(R-7)}$$

The kinetics for this reaction, listed in Table 2, are taken to be the same as given by Tarver and McGuire.[2] Briefly, the HMX mechanism will be applied to the ODTX and hot cell experiment by suppressing the sublimation reactions (R-1) and (R-3) and adding the highly exothermic gas-phase reaction (R-7). For the present paper, reactions (R-1) and (R-3) were suppressed by using a high activation energy. The pressure dependence of the sublimation reactions could be added for a more general mechanism.

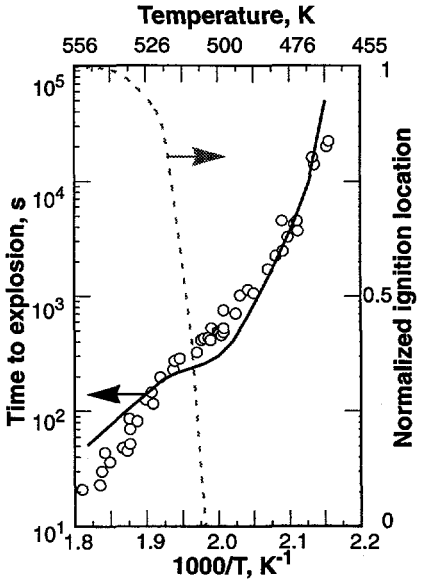

Fig. 5. Calculated (line) and experimental time (circle) to failure for 1.27 cm diameter spheres of HMX.

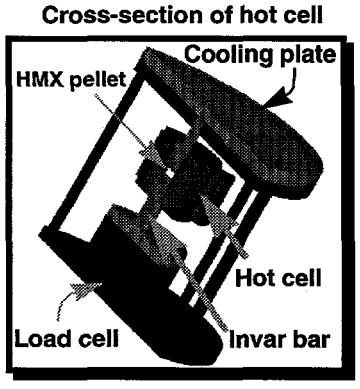

Fig. 6. Cross-section of the hot cell experiment showing major components.

ODTX SIMULATION

In the spherical ODTX experiments, Tarver and McGuire[2] modeled preheated aluminum anvils confining 1.27 cm diameter spherical samples of explosive. Heaters controlled the temperature of the anvils to ±0.2 K, and the primary measurement was the time to "explosion" which represented confinement failure. The anvil confinement is sealed to 1500 atm.

The predictions (lines) and experimental (symbols) ODTX results for HMX are shown in Fig. 5. All thermal parameters were taken unchanged from Reference 2. Typically, the logarithm of time to confinement failure versus the reciprocal of the surface temperature is linear over a large region, but sharply bends upward near the critical temperature The predicted time to explosion adequately matches the time to explosion data using the global HMX mechanism. The change in slope of the calculated time to ignition between 526 K and 500 K results from migration of the ignition location from the edge to the center of the HMX.

HOT CELL EXPERIMENT

The ODTX simulation demonstrates that the HMX mechanism can predict the time to reaction provided the sublimation reactions are suppressed and the gas-phase reactions are included. To calculate the response of the energetic material beyond ignition, the state of the degraded material is required. Dynamic, post-ignition burn rates depend on the amount of material that has decomposed, the location of material decomposition, the temperature of the degraded material, morphological changes, preignition stress states, and confinement integrity.

The REP constitutive model[4] couples the thermal/chemical behavior to the mechanical behavior of HMX to determine the degraded state of the energetic material. To validate and calibrate the REP constitutive model, Renlund et al.[3] have developed a small scale experiment which can be used to measure the rate of pressurization of confined energetic materials subjected to a controlled thermal field. A schematic of the hot cell experiment is shown in Fig. 6.A. The HMX was confined in a block of stainless steel (hot cell) and two opposing invar bars. O-rings were used to prevent gases from leaking out of the hot cell. A stainless steel cage composed of two plates and six bolts, supports the load cell and the HMX confinement apparatus. Experimental data from the hot cell containing HMX is shown in Fig. 6.B. The linear increase in stress measured by the load cell between 35 to 50 minutes represents thermal expansion of the invar bar and HMX. The nonlinear behavior between 50 and 60 minutes is thought to be associated with HMX phase transformations. The increase in load from 90 minutes to the end of the experiment is postulated to be induced by gas formation. The experiment ended when the O-ring failed near 110 minutes.

The hot cell data show an increase in axial force, due to thermal expansion, gas formation, and phase change; as well as a decrease in axial force (relaxation) possibly due to phase change induced viscoplastic behavior. The primary independent REP variables are temperature and reacted gas fraction histories. The reacted gas fraction

is the amount of solid material that has been converted to gaseous products. The ability to predict the degraded state of HMX in cookoff experiments is dependent on the ability to predict the reacted gas fraction accurately. Fig. 6.B illustrates the predicted reacted gas fraction for HMX experiment #26 using the 5 step mechanism represented by reactions R-2, R-4, R-5, R-6, and R-7; the 3-step Tarver and McGuire mechanism; and an estimate using the BKW equation-of-state (EOS).[4] The 5-step and 3-step mechanism give similar predictions of the reacted gas fraction.

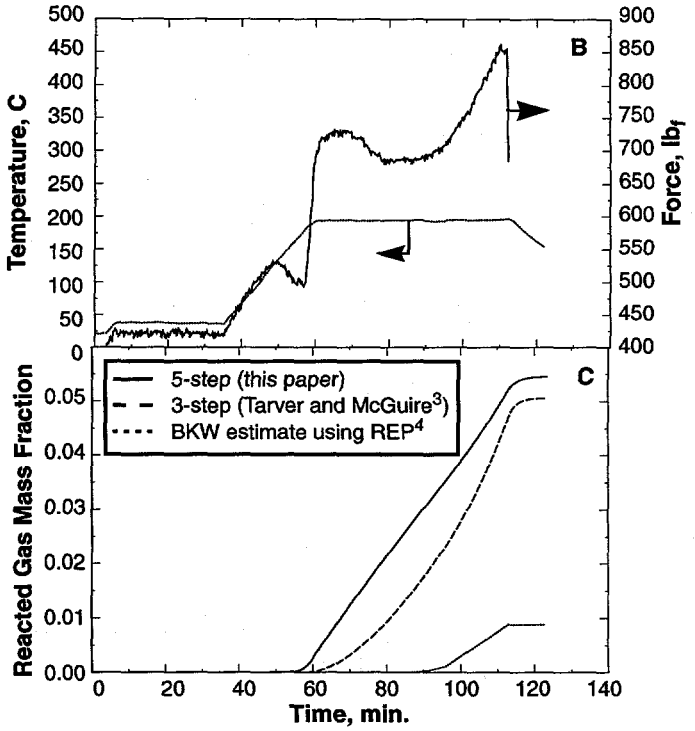

Fig. 7. A) HMX pellet temperature history and axial load history as measured in the HMX hot cell experiment, B) prediction of the reacted gas fraction.

The BKW estimate of the HMX reacted gas fraction is based on using the measured force increase between 85 and 110 minutes. The average reacted gas molecular weight and BKW covolume was assumed to be 30 g/mol and 394, respectively, as based on equilibrium calculations. The volume of the gap between the invar rods and the hot cell was estimated with a quasistatics mechanics code,[4] using slidelines (14 μm gap) to be roughly 1% of the original pellet volume. The gap volume was calculated based on the distance from the top of the pellet to the confining O-ring, 0.1575 cm. The HMX pellet radius was assumed to be the same as the inner bore radius of the stainless steel hot cell. The mechanical behavior of the HMX pellet was based on the REP constitutive model which uses the Mie-Grüneisen EOS for the solid HMX. The gas fraction predicted with the BKW model is significantly different than either the 5-step model or the 3-step model as shown in Fig. 6.C. However, the BKW prediction would be closer to the 5-step and 3-step prediction by assuming an average gas molecular weight of about 58 g/mol. Also. the initial and final recovered mass of the HMX pellet for run #26 was 0.1910 g and 0.1516 g, respectively; indicating a final reacted gas fraction of 0.16. However, complete recovery of HMX pellet is difficult due to the small size of the HMX pellet. The actual reacted gas fraction will be measured in future hot cell experiments.

SUMMARY AND CONCLUSIONS

The state of HMX during cookoff depends on complex decomposition pathways that include formation of light gases, heavy gases, sublimation of HMX, sublimation of the mononitroso analog of HMX, and gas-phase reactions. The kinetic mechanism for these various pathways are likely different for the two primary solid phases of HMX: β-HMX and δ-HMX. In the STMBMS experiments, β-HMX eventually is converted to δ-HMX. To separate the kinetic behavior of β-HMX from δ-HMX, kinetic rate parameters for a 6-step mechanism were obtained from STMBMS data after significant weight loss was observed. The parameters for the experimentally-based 6-step mechanism were obtained by minimizing the normalized squared difference between predicted product distributions and the STMBMS data at 210.5 C, 235.2 C, and 226.5 C. The object oriented optimization toolkit, DAKOTA,[8] was used to minimize the objective function. The apparent activation energies were constrained to be greater than the weakest bond in the HMX molecule. Two of the six reactions were assumed to be zero order sublimation reactions. The remaining four reaction orders were constrained to be close to unity. The computed solid mass fraction was higher than measure values taken at 210.5 and lower than measured values at 226.5 C and 235.2 C.

The HMX mechanism was deduced from STMBMS data taken near atmospheric pressure with the decomposition products exiting the reaction vessel without significant gas-phase reaction. The mechanism was applied to the ODTX experiment[2] confined to 1500 atm and the hot cell experiment[3] confined between 600 atm and 1200 atm. The gases do not leave the reaction vessel in these heavily confined experiments. To account for higher pressure and confined gases, the sublimation reactions were suppressed and the gas-phase reaction of N_2O with H_2CO to form H_2O, N_2, and CO was added to the reaction set. The modified HMX mechanism, providing for suppressed sublimation and gas-phase reactions, gave adequate agreement between predicted and measured time to reaction for the ODTX experiments.

The modified HMX mechanism was also applied to the hot cell experiment to determine the reacted gas fraction. The final predicted reacted gas fraction for the modified HMX mechanism, the Tarver and McGuire mechanism, and an estimate using the BKW-EOS was 0.0545, 0.0506, and 0.0090. The reacted gas fraction calculated from pellet recovery is approximately 0.16 which is thought to be an upper bound due to recovery difficulties. The similarity between the modified mechanism and the Tarver and McGuire mechanism may be a result of using the same gas-phase chemistry. More experiments are needed to determine if the predicted extent of reaction is adequate.

The response of an energetic material following ignition cannot be sufficiently determined if the extent of reaction at ignition is unknown. This paper has discussed several advances in understanding thermally decomposing HMX near atmospheric pressure and at high pressure under confinement. Additional experiments and improved modeling are necessary to advance our understanding of decomposition during cookoff. The effect of particle size distribution, measurement of the reacted gas fraction, and high pressure phase behavior should be investigated experimentally.

ACKNOWLEDGMENT

I would like to express my appreciation to Mel Baer, Rich Behrens, and Leanna Minier for several useful discussions during the progress of the work. I would like to thank Mike Eldred for his help with DAKOTA[8] and Bob Schmitt for help in interfacing TREX[9] with DAKOTA.[8]

REFERENCES

1. Behrens, R., Jr., "Thermal Decomposition of Energetic Materials: Temporal Behaviors of the Rates of Formation of the Gaseous Pyrolysis Products from Condensed-Phase Decomposition of Octahydro-1,3,5,7-tetranitro-1,3,5,7-tetrazocine," *J. Phys. Chem.*, **94**, 6706 (1990).

2. Tarver, C. M., Chidester, S. K., and Nichols, A. L., III, "Critical Conditions for Impact- and Shock-Induced Hot Spots in Solid Explosives," *J. Phys. Chem.*,**100**, 5794 (1996). See also McGuire, R. R. and Tarver, C. M., "Chemical Decomposition Models for the Thermal Explosion of Confined HMX, TATB, RDX, and TNT Explosives," *Seventh Symposium (International) on Detonation*, NSWC MP 82-334, Naval Surface Weapons Center, White Oak, Maryland, 56 (1981).

3. Renlund, A., Miller, J. C., Hobbs, M. L., and Baer, M. R., "Experimental and Analytical Characterization of Thermally Degraded Energetic Materials," *JANNAF Propulsion Systems Hazards Subcommittee (PSHS) Meeting*, NASA Marshall Space Flight Center, Huntsville, AL (1995).

4. Hobbs, M. L., Schmitt, R. G., Renlund, A. M., "Analysis of Thermally-Degrading, Confined HMX," *1996 JANNAF Propulsion Systems Hazards Subcommittee Meeting*, Naval Postgraduate School, Monterey, CA (4-8 Oct 1996).

5. Baer, M. R., Kipp, M. E., Hobbs, M. L., and Schmitt, R. G., "Toward Assessing the Violence of Reaction During Cookoff of Confined Energetic Materials," *1996 JANNAF Propulsion Systems Hazards Subcommittee Meeting*, Naval Postgraduate School, Monterey, CA (4-8 Oct 1996).

6. Behrens, R. and Bulusu, S., "The Importance of Mononitroso Analogues of Cyclic Nitramines to the Assessment of the Safety of HMX-Based Propellants and Explosives," *Fourth International Symposium on Special Topics in Propulsion*, Stockholm, Sweden (1996).

7. Behrens, R., personal communication, Sandia National Laboratories, Albuquerque, NM (Oct. 23, 1996).

8. Eldred, M. S., Hart, W. E., Bohnhoff, W. J., Romero, V. J., Hutchinson, S. A., and Salinger, A. G., "Utilizing Object-Oriented Design to Build Advanced Optimization Strategies with Generic Implementation," AAIAA-4164 in *Proceedings of the 6th AIAA/USAF/NASA/ISSMO Symposium on Multidisciplinary Analysis and Optimization*, Bellevue, WA, 1568 (Sept. 4-6, 1996). See also Eldred, M. S., Outka, D. E., Bohnhoff, W. J., Witkowski, W. R., Romero, V. J., Ponslet, E. R., and Chen, K. S., "Optimization of Complex Mechanics Simulations with Object-Oriented Software Design," *Computer Modeling and Simulation in Engineering*, **1**,3 (August 1996).

9. Hobbs, M. L., Baer, M. R., and Gross, R. J., "Thermal-Chemical-Mechanical Cookoff Modeling," *JANNAF Propulsion Systems Hazards Subcommittee Meeting*, CPIA Publication 615, San Diego, CA, 311 (1994).

10. Sjaardema, G. D., "APREPRO: An Algebraic Preprocessor for Parameterizing Finite Element Analyses," SAND92-2291, UC-705, Sandia National Laboratories, Albuquerque, NM (1994).

11. Anderson, G. and Anderson, P., *The UNIX C Shell Field Guide*, Prentice Hall, Englewood Cliffs, NJ (1986).

12. Erickson, K. L., personal communication, Sandia National Laboratories, Albuquerque, NM (1996).